ACOUSTICS 2017 PERTH
SOUND, SCIENCE AND SOCIETY

Acoustic Absorption of Porous Materials Produced by Additive Manufacturing with Varying Geometries

Chaoyang Jiang (1), Danielle Moreau (1) and Con Doolan (1)

(1) School of Mechanical and Manufacturing Engineering, UNSW Sydney, NSW, Australia

ABSTRACT

This paper investigates the sound absorption capability of porous materials produced by additive manufacturing (sometimes known as 3D printing) with different geometrical parameters, where the porosity Φ, hole diameter d_0, specimen thickness h and aspect ratio d_0/h are chosen for parametric study. The sound absorption coefficient of the specimens is experimentally measured by using a two-microphone impedance tube and the results indicate that the frequency of the peak absorption coefficient varies with porosity and the peak value is insensitive to the diameter of the holes but strongly correlated to the aspect ratio. Finally, the selection criterion of geometric parameters of 3D printed porous materials is established for achieving maximum sound absorption at a certain frequency.

1 INTRODUCTION

Porous materials have been widely used in the noise control of buildings, vehicles, aircraft, etc. The tortuous pores can dissipate the acoustic wave energy by viscous dissipation and thermal conductivity. In recent years, intensive research has been conducted to evaluate the sound absorption capability of different innovative porous materials. In general, those studies could be grouped into two categories: metallic porous and non-metallic porous materials.

In terms of metallic porous materials, Xie et al. (2004) investigated the sound absorption ability of lotus-type porous copper with porosity ranging from 43~52%. Hur et al. (2005) examined the sound absorption coefficient of aluminium fibre and foam. The acoustic absorption performance of porous fibrous metal at high sound power levels was investigated by Wang et al. (2009). Pannert et al. (2009) measured the absorption coefficient of porous metal with hollow sphere structure; JingFeng et al. (2014) characterized the absorption capability of multilayer aluminium foam with airgaps of different thickness; Sun et al. (2015) prepared steel slag porous material and examined its acoustic properties; Ru et al. (2015) measured the sound absorption coefficient of porous copper prepared by resin curing and a foaming method. For non-metallic porous materials, the acoustic properties of porous ceramic materials were characterized in (Cuiyun et al. 2012, Wu et al. 2014), showing broadband sound absorption above 500Hz. The acoustic properties of polyolefin-based porous materials and a novel multilayer poly foam were investigated by Álvarez-Láinez et al. (2014) and Zhao et al. (2015) respectively. With growing concern about a green and sustainable environment, sound absorption bio materials have drawn much attention. The sound absorption performance of tea-leaf-fibre, vegetable particle materials and luffa fibre have been examined in (Ersoy et al. 2009), (Glé et al. 2011) and (Koruk et al. 2015) respectively, indicating that bio materials indeed have the potential to act as sound absorbers. In summary, for various innovative porous materials reported in previous studies, good sound absorption coefficient could be achieved over frequencies ranging from 500Hz to 6000Hz. However, for the noise control of a specific application, it could be considered challenging to customize the frequency characteristics of sound absorption coefficient for the aforementioned porous materials.

More recently, for the ease of customizing the internal structure, additive manufacturing technology (otherwise known as 3D printing) has been applied to the preparation of sound absorbing materials. 3D printed continuously graded phononic crystals have been acoustically characterized by Zhang et al. (2016), showing a potential in broadband noise absorption, especially at lower frequencies over 1350Hz to 3000Hz. Liu et al. (2016) investigated the acoustic properties of 3D printed polycarbonate porous materials, indicating a high sound absorption coefficient could be achieved by the proposed materials. The peak absorption frequency of this 3D printed material could be shifted to a desired range using an airgap configuration.

In this study, inspired by micro perforation panel theory proposed by (Maa 1975, 1998), a series of open-cell porous materials with straight micro-tube-shape holes have been fabricated by additive manufacturing. The acoustic properties of the proposed materials with varying geometries have been measured. Furthermore, the geometry design criteria for achieving maximum sound absorption over a certain frequency range have been discussed.

2 METHODOLOGY

2.1 Specimens

In this study, all specimens are made of 3D printing material Visijet M3 supplied by 3D Systems Inc.. This material has a liquid density of 1.02 g/cm^3 at 80 ºC; a tensile strength of 42.4 MPa; a tensile modulus of 1463 MPa and a flexural strength of 49 MPa. A high-definition professional 3D printer Projet 3500 HD*Max* was adopted for specimen fabrication. All specimens are printed with a layer resolution of 16 µm and an accuracy of 0.025-0.05mm per 25.4 mm of part dimension. The structure of test specimens is shown in Figure 1, the geometries of these specimens are characterized by pore diameter d_0, thickness h, aspect ratio $\gamma = d_0/h$ and porosity $\Phi = V_v/V_T$, where V_v is the volume of void-space and V_T is the total volume of material. The acoustic properties of ten porous specimens and three reference specimens were measured, where the reference specimens were used to evaluate the effectiveness of the porous specimens. All cylinder specimens have a diameter of D = 29 mm. For the ten porous specimens P1 ~ P10, the porosity Φ ranges from 5.35% to 11.53%; hole diameter d_o ranges from 0.6 mm to 1mm and thickness h ranges from 5mm to 10mm. For the two reference specimens R1 and R2, they are non-porous cylinders with a diameter D = 29mm and thickness of 5mm and 10mm respectively. R3 is All geometric detailed of these twelve specimens are listed in Table 1.

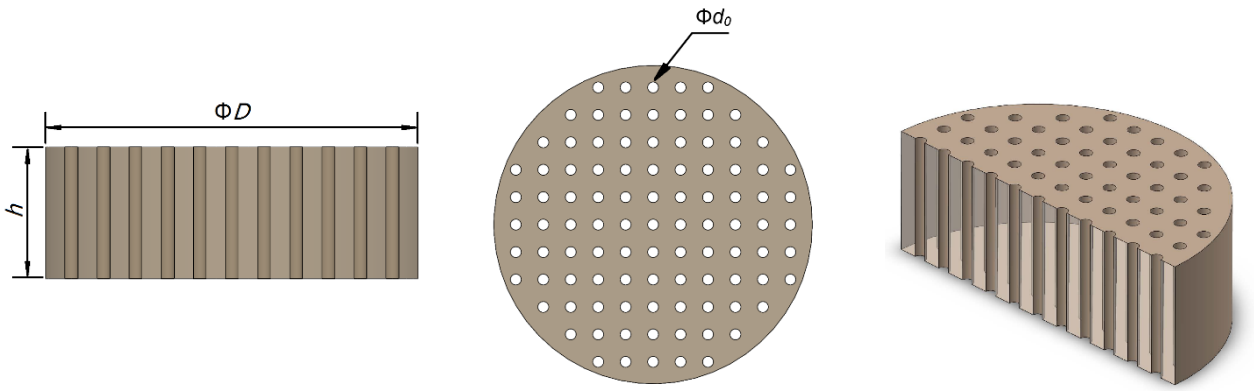

(a)

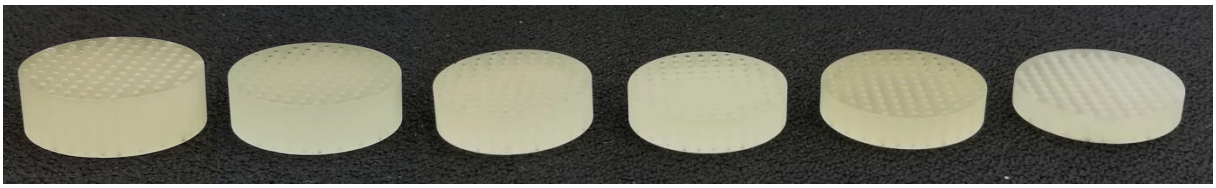

(b)

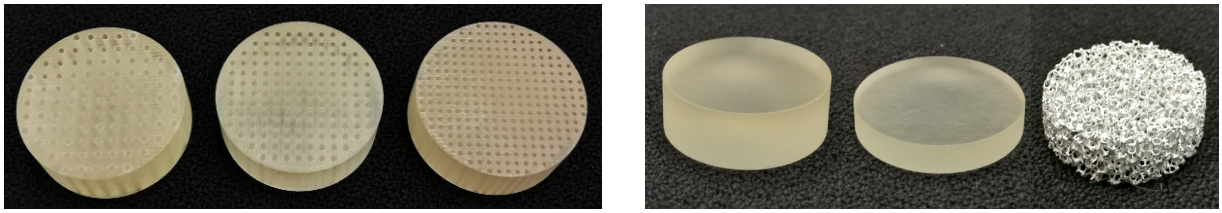

(c) (d)

Figure 1: Geometry of 3D printed specimens. (a) Specimen structure; (b) Specimens with different thickness h; (c) Specimens with different hole diameter d_0; (d) Reference specimens: R1(3D printed; solid; h=10mm), R2(3D printed; solid; h=5mm) and R3(Aluminium foam; porosity Φ=92~94%)

Table 1: Geometric properties of test specimens

Specimen	No. Holes	Hole Diameter d_0 (mm)	Porosity Φ (%)	Thickness h (mm)	Aspect Ratio γ
P1	97	1	11.53	10	0.1
P2	69	1	8.20	10	0.1
P3	45	1	5.35	10	0.1
P4	146	0.8	11.11	10	0.08
P5	269	0.6	11.51	10	0.06
P6	97	1	11.53	9	0.111
P7	97	1	11.53	8	0.125
P8	97	1	11.53	7	0.143
P9	97	1	11.53	6	0.167
P10	97	1	11.53	5	0.2
R1	0	0	0	10	n/a
R2	0	0	0	5	n/a
R3	n/a	n/a	92~94	10	n/a

2.2 Measurement setup and theoretical background

The acoustic properties of the 3D printed specimens were measured by a two-microphone impedance tube B&K type 4206. It consists of a solid anodised aluminium tube with a diameter of 29 mm. The specimens were held at a rigid termination at one end of the tube. A loudspeaker was situated at the other end acting as sound source. Two microphones were positioned at two different positions on the top of the tube to measure the acoustic properties of the specimens.

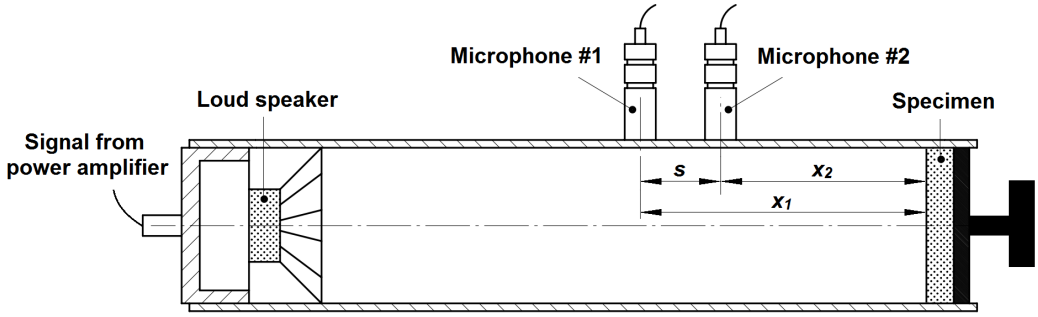

(a)

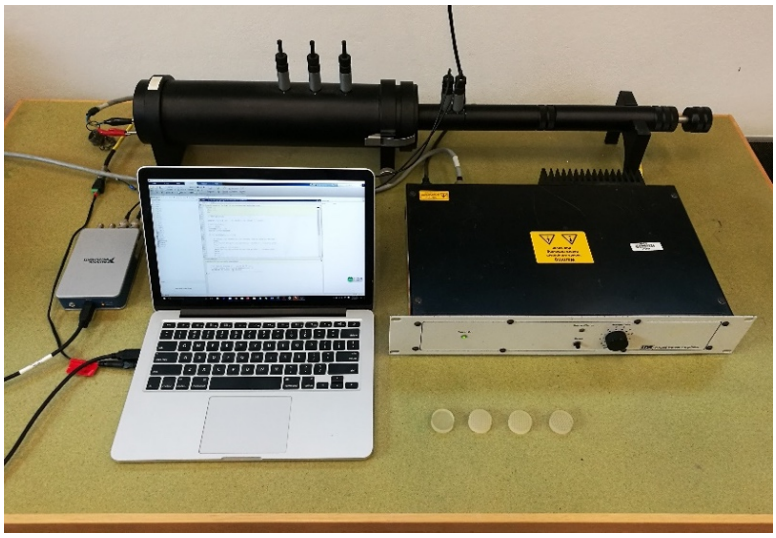

(b)

Figure 2: (a) Schematic of impedance tube; (b) measurement setup *in-situ*

The acoustic measurement is based transfer function method introduced by Chung et al. (1980). As shown in Figure 2(a), the test specimen is fixed at one end, the distance from the test specimen front face to the further microphone and closer microphone are denoted as x_1 and x_2, distance between two microphone is denoted as s= x_1- x_2. The transfer function for the incident wave H_I and for the reflected wave H_R are

$$H_I = \frac{p_{2I}}{p_{1I}} = e^{-jk_0(x_1-x_2)} = e^{-jk_0 s}, \quad (1)$$

$$H_R = \frac{p_{2R}}{p_{1R}} = e^{-jk_0(x_1-x_2)} = e^{jk_0 s}, \quad (2)$$

where p_{iI} and p_{iR} are incident and reflected sound pressure in the position of microphone i, k_0 is the wave number k_0=2πf/c. The transfer function H_{12} can be determined by

$$H_{12} = \frac{p_2}{p_1} = \frac{e^{jk_0x_2}+re^{-jk_0x_2}}{e^{jk_0x_1}+re^{-jk_0x_1}}, \quad (3)$$

and complex sound reflection coefficient r, complex acoustic impedance Z and sound absorption coefficient α can be determined by

$$r = \frac{H_{12}-H_I}{H_R-H_{12}} e^{2jk_0x_1}, \quad (4)$$

$$Z = \frac{1+r}{1-r}\rho c, \quad (5)$$

$$\alpha = 1 - |r|^2. \quad (6)$$

Measurement setup *in-situ* is shown in Figure 2(b), a B&K LDS PA25E power amlifier and a loud speaker act as the sound source, two G.R.A.S Type 40PH Free-field micophones are used to measure sound pressure, a laptop and a NI 9234 CompactDAQ 24 bit are used to generate the source signal and collect measured data respectively. In this experiment, the complex sound reflection coefficient, acoustic impedance and sound absorption coefficient of twelve specimens have been examined.

3 RESULTS AND DISCUSSION

3.1 Effect of porosity

Figure 3 presents the comparison of sound absorption coefficients of specimens P1, P2, P3 and reference specimen R1 (solid). For P1, P2 and P3, they have the same thickness h and same hole diameter d_0 but different porosity resulting from different hole numbers. The porosities for specimens P1, P2 and P3 are 11.53%, 8.20% and 5.35% respectively. As shown in Figure 3, for frequencies lower than 3800Hz, the specimens have very similar sound absorption coefficients (less than 0.2) which are relatively low and could be considered inefficient for sound absorption. For frequencies higher than 3600Hz, the sound absorption coefficients of porous specimens are significantly greater than that of solid reference specimen R1, indicating that the sound absorption resulting from porous structures is efficient for higher frequencies from 3600Hz to 6400Hz. For the sound absorption coefficient of porous specimens over 500Hz to 6400Hz, the peak amplitude varies from 0.79 to 0.99 and the peak absorption frequencies range from 5400Hz to 6200Hz. These specimens have showed good acoustic absorption performance over 5000Hz. Furthermore, it is noticeable that the peak frequency and amplitude of the absorption coefficient has shown a tendency to decrease with decreasing porosity. Therefore, for noise control over a specific frequency range, a potential strategy of shifting the peak sound absorption coefficient is to optimally adjust the porosity distribution.

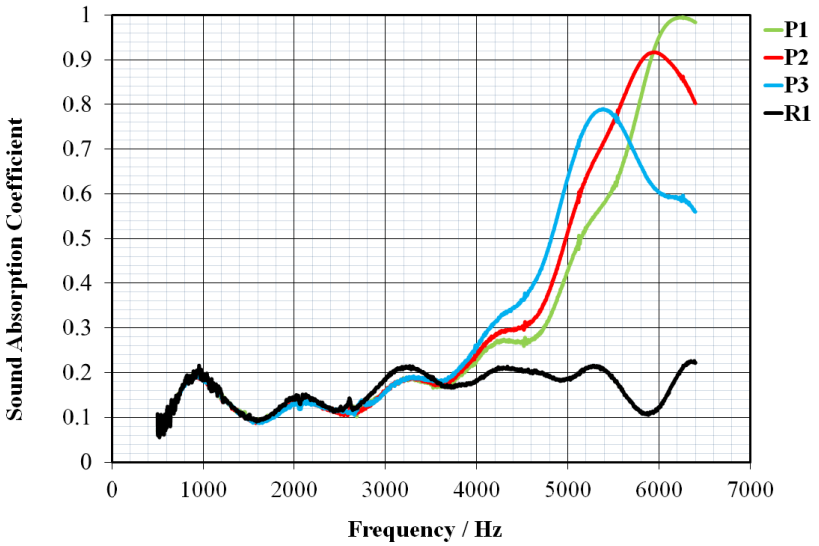

Figure 3: Sound absorption coefficients of reference specimen R1(solid, Φ=0) and specimens with same thickness h, same hole diameter d_0 and different porosity Φ. P1: Φ=11.53%; P2: Φ=8.20%; P3: Φ=5.35%.

3.2 Effect of aspect ratio

Figure 4(a) shows the sound absorption performance of specimens P1, P4, P5 and reference specimen R1. For porous specimens, they have almost identical porosities, which are 11.53%, 11.11% and 11.51% for P1, P4 and P5 respectively. The most significant difference between these specimens is that they have different hole diameter d_0, which are 1mm, 0.8mm and 0.6mm for P1, P4 and P5, respectively. The results presented in Figure 4(a) show that for these three porous specimens, the frequency characteristics of their sound absorption coefficients are similar, hence the dependency of porosity on the frequency characteristic of 3D printed materials is reasonably independent of hole diameter. It can also be found that the peak values of the sound absorption coefficient are similar, ranging from 0.96 to 0.99. To be noticed, the comparison between porous specimens and reference specimen has also shown that porous structures are efficient for sound absorption at higher frequencies ranging from 3600Hz to 6400Hz.

Figure 4(b) shows the comparison of sound absorption coefficient curves of specimens with same porosity and different thickness h. It could be found that the trends of their sound absorption curves are considerably similar. However, their amplitudes varied significantly from 0.24 to 0.99, indicating the strong dependency of sound absorption amplitude and the geometry of the micro tubes inside these porous materials.

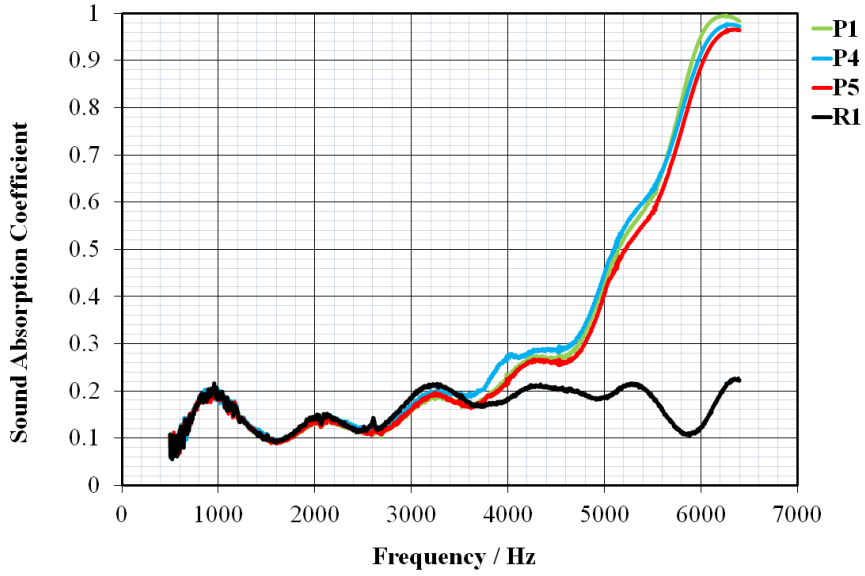

(a)

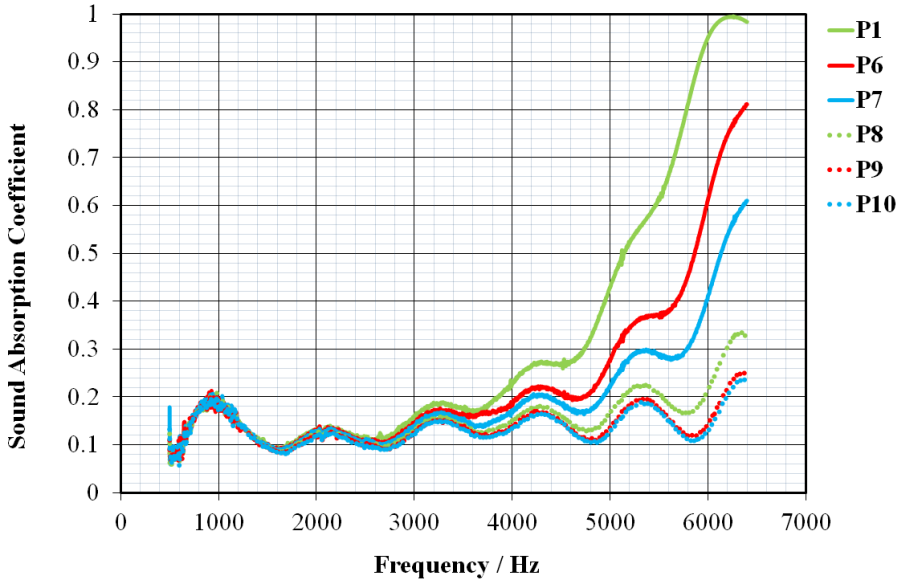

(b)

Figure 4: Sound absorption coefficients of reference specimen R1(solid, Φ=0), specimens with same porosity (11.5%) and different thickness h or different hole diameter d_0. (a) Reference specimen and specimens with different hole diameter d_0; (b) specimens with different thickness h.

For a certain cylinder-shape micro tube inside these porous materials, its geometry can be described by the aspect ratio $\gamma = d_0/h$. Figure 5 shows the variation of peak sound absorption coefficients with aspect ratio. The peak absorption coefficient first increases with aspect ratio from γ = 0.06 to 0.1 and peaks at around γ = 0.1 with the value of α = 0.99, then quickly decreases to around α = 0.3 when the aspect ratio increases from 0.1 to 0.16, and finally gently approaches an asymptotic value of α = 0.25 as the aspect ratio increases further. Since porosity is the most significant parameter affecting acoustic absorption, it can be concluded that the maximum sound absorption performance for this type of material with a certain porosity may be achieved by optimal design of the hole aspect ratio.

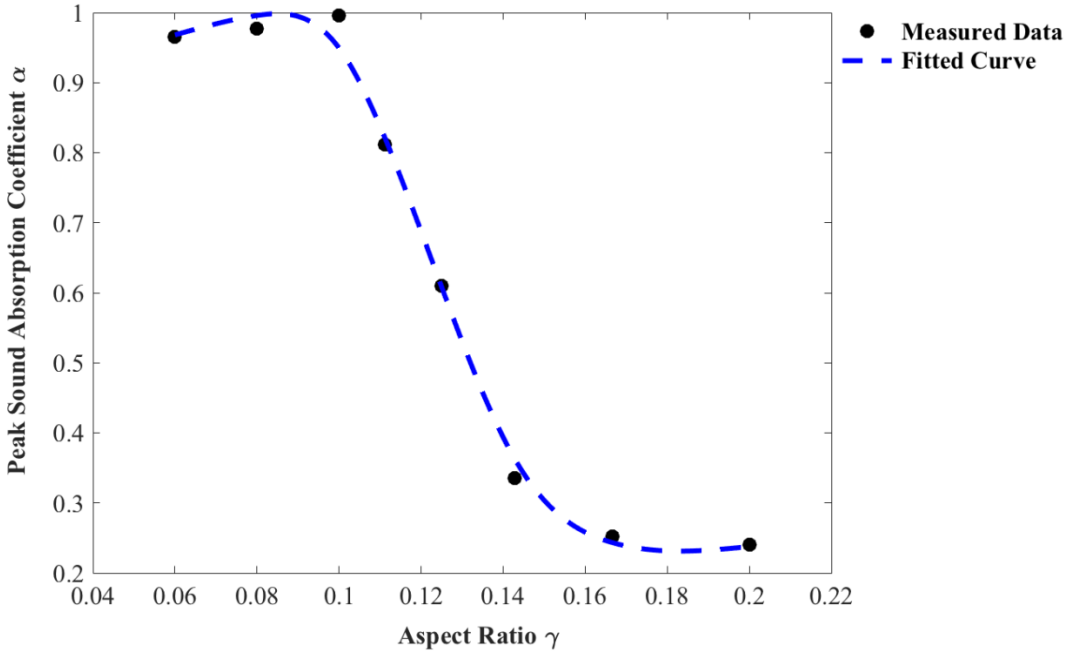

Figure 5: Relationship between aspect ratio γ and peak sound absorption coefficient α.

The comparison of sound absorption coefficients between porous specimens and reference specimens is shown in Figure 6. Figure 6(a) presents the comparison between P1, R1and R3, that both have thickness of 10mm. For 3D printed specimens P1 and R1, their sound absorption curves are very similar under 3600Hz, which again indicates that the holes inside this material are inefficient in absorbing sound over 500Hz to 3600Hz. For frequencies ranging from 3600Hz to 6400Hz, the sound absorption performance of the porous specimen is much better than that of the solid specimen. Moreover, compared with aluminium foam R3, the 3D printed porous specimen P1 is much more efficient in sound absorption over 2800Hz to 6400Hz.

Figure 6(b) shows the sound absorption coefficient of P10 and R2, that both have thickness of 5mm. It can be seen that the trends of their sound absorption curves are also similar, and the overall sound absorption performance of the porous specimen is even worse than the solid reference specimen. It might result from the high aspect ratio of the holes, making the viscous dissipation and thermal conductivity inefficient in dissipating acoustic energy. Summarized from the results presented in Figure 4, 5 and 6, for the proposed 3D printed porous materials with a porosity of 11.53%, the aspect ratio of the holes inside the material should be less than 0.14 to be effective in normal-incident sound absorption. In general, it could be deduced that for such materials with a certain porosity, an optimal aspect ratio to achieve maximum sound absorption and a maximum aspect ratio for the materials to be effective in sound absorption are existed. To optimally design the geometry of this type of material to achieve the maximum sound absorption performance for a specific application, porosity and hole aspect ratio are two crucial parameters that should be determined.

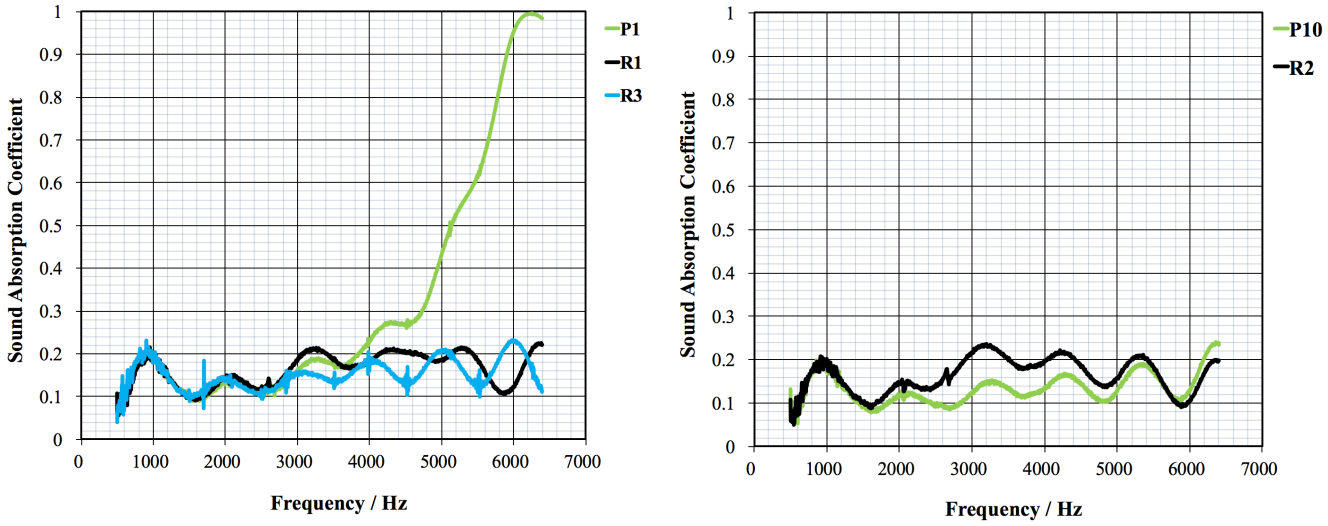

(a) (b)

Figure 6: Comparison of sound absorption coefficients of porous specimens (Φ=11.53%) and reference specimens. (a) Specimens with thickness h=10mm: P1, R1 and R3; (b) specimens with thickness h=5mm: P10 and R2.

4 CONCLUSIONS

This paper investigated the feasibility of fabricating 3D printed materials with micro-tube-shaped holes using additive manufacturing and evaluated their acoustic properties. A series of such 3D printed materials have been fabricated by a professional 3D printer, and their sound absorption performance has been measured using an impedance tube. The results have shown that the peak sound absorption coefficients ranging from 0.24 to 0.99 can be achieved by test specimens, and they are examined to have good sound absorption performance over higher frequencies ranging from 4800Hz to 6400Hz. Based on the experimental data obtained in this work, it could be concluded that the frequency characteristics of 3D printed materials with mirco-tube-shape holes are correlated to the porosity of the material. Furthermore, to achieve maximum sound absorption for noise over a desired frequency range, the following geometric design criterion for proposed 3D printed porous materials have been discussed and established: 1) the peak frequency of sound absorption coefficient can be shifted to lower frequencies by increasing porosity; 2) for materials with a certain porosity, the amplitude of their sound absorption coefficient strongly correlated with the hole aspect ratio, and the maximum sound absorption coefficient can be achieved by selecting an optimal hole aspect ratio. However, more experimental work is still needed to establish a more comprehensive database for the application of this type of 3D printed porous material. A promising further study will focus on extending proposed materials to noise control of aeroacoustic applications.

ACKNOWLEDGEMENTS

The authors would like to thank Chinese Scholarship Council for providing the PhD scholarship.

REFERENCES

Álvarez-Láinez, Mónica, Miguel Angel Rodríguez-Pérez, and Jose Antonio de Saja. 2014. "Acoustic absorption coefficient of open-cell polyolefin-based foams." *Materials Letters* 121:26-30. doi: 10.1016/j.matlet.2014.01.061.

Chung, J. Y., and D. A. Blaser. 1980. "Transfer function method of measuring in ‐ duct acoustic properties. I. Theory." *The Journal of the Acoustical Society of America* 68 (3):907-913. doi: 10.1121/1.384778.

Cuiyun, Duan, Cui Guang, Xu Xinbang, and Liu Peisheng. 2012. "Sound absorption characteristics of a high-temperature sintering porous ceramic material." *Applied Acoustics* 73 (9):865-871. doi: 10.1016/j.apacoust.2012.01.004.

Ersoy, Sezgin, and Haluk Küçük. 2009. "Investigation of industrial tea-leaf-fibre waste material for its sound absorption properties." *Applied Acoustics* 70 (1):215-220. doi: 10.1016/j.apacoust.2007.12.005.

Glé, P., E. Gourdon, and L. Arnaud. 2011. "Acoustical properties of materials made of vegetable particles with several scales of porosity." *Applied Acoustics* 72 (5):249-259. doi: 10.1016/j.apacoust.2010.11.003.

Hur, Bo Young, Bu Keoun Park, Dong-In Ha, and Yong Su Um. 2005. "Sound absorption properties of fiber and porous materials." Materials Science Forum.

JingFeng, N., and Z. GuiPing. 2014. "Sound absorption characteristics of multilayer porous metal materials backed with an air gap." *Journal of Vibration and Control* 22 (12):2861-2872. doi: 10.1177/1077546314548086.

Koruk, Hasan, and Garip Genc. 2015. "Investigation of the acoustic properties of bio luffa fiber and composite materials." *Materials Letters* 157:166-168. doi: 10.1016/j.matlet.2015.05.071.

Liu, Zhengqing, Jiaxing Zhan, Mohammad Fard, and John Laurence Davy. 2016. "Acoustic properties of a porous polycarbonate material produced by additive manufacturing." *Materials Letters* 181:296-299. doi: 10.1016/j.matlet.2016.06.045.

Maa, Dah-You. 1975. "Theory and design of microperforated panel sound-absorbing constructions." *Scientia Sinica* 18 (1):55-71.

Maa, Dah-You. 1998. "Potential of microperforated panel absorber." *The Journal of the Acoustical Society of America* 104 (5):2861-2866. doi: 10.1121/1.423870.

Pannert, W., R. Winkler, and M. Merkel. 2009. "On the acoustical properties of metallic hollow sphere structures (MHSS)." *Materials Letters* 63 (13-14):1121-1124. doi: 10.1016/j.matlet.2008.10.063.

Ru, Jinming, Bo Kong, Yaoguang Liu, Xiaolin Wang, Tongxiang Fan, and Di Zhang. 2015. "Microstructure and sound absorption of porous copper prepared by resin curing and foaming method." *Materials Letters* 139:318-321. doi: 10.1016/j.matlet.2014.09.084.

Sun, P., and Z. Guo. 2015. "Preparation of steel slag porous sound-absorbing material using coal powder as pore former." *J Environ Sci (China)* 36:67-75. doi: 10.1016/j.jes.2015.04.010.

Wang, X., F. Peng, and B. Chang. 2009. "Sound absorption of porous metals at high sound pressure levels." *J Acoust Soc Am* 126 (2):EL55-61. doi: 10.1121/1.3162828.

Wu, Gaohui, Ruifeng Li, Yu Yuan, Longtao Jiang, and Dongli Sun. 2014. "Sound absorption properties of ceramic hollow sphere structures with micro-sized open cell." *Materials Letters* 134:268-271. doi: 10.1016/j.matlet.2014.07.082.

Xie, Zhenkai, Teruyuki Ikeda, Yosiyuki Okuda, and Hideo Nakajima. 2004. "Sound absorption characteristics of lotus-type porous copper fabricated by unidirectional solidification." *Materials Science and Engineering: A* 386 (1):390-395. doi: http://dx.doi.org/10.1016/j.msea.2004.07.058.

Zhang, X. H., Z. G. Qu, X. C. He, and D. L. Lu. 2016. "Experimental study on the sound absorption characteristics of continuously graded phononic crystals." *AIP Advances* 6 (10):105205. doi: 10.1063/1.4965923.

Zhao, Tianbao, Mingtao Yang, Hong Wu, Shaoyun Guo, Xiaojie Sun, and Wenbin Liang. 2015. "Preparation of a new foam/film structure poly (ethylene-co-octene) foam materials and its sound absorption properties." *Materials Letters* 139:275-278. doi: 10.1016/j.matlet.2014.10.061.